The Bowed String As We Know It Today

J. Woodhouse, P. M. Galluzzo
Cambridge University Engineering Department, Trumpington Street, Cambridge CB2 1PZ, UK.
jw12@eng.cam.ac.uk

Summary

The vibration of a bowed string has been studied since the 19th century, and today this problem is the only example of vibration excited by friction which can claim to be well understood. Modern theoretical models embody many of the complicating features of real strings, instruments and bows, and detailed comparisons with experimental studies are allowing fine tuning of the models to take place. The models can be used to explore questions directly relevant to instrument makers and players. The main unresolved question at present concerns the description of the frictional behaviour of rosin, since recent results have shown that the friction model used in most earlier studies is incorrect. Better friction models are being developed in current research.

1. Introduction

Modern research on the physics of the bowed string began with the discovery by Helmholtz, 140 years ago [1], that a string vibrates in a "V-shape" when bowed in the normal way. The vertex of the V travels back and forth along the string as illustrated in Figure 1. Each time this "Helmholtz corner" passes the bow, it triggers a transition between sticking and sliding friction: the string sticks to the bow while the corner travels from bow to finger and back, and it slips along the bow hairs while the corner travels to the bridge and back. This "Helmholtz motion" is the goal for the vast majority of musical bow-strokes.

With this in mind, it is possible to distinguish two types of quality which contribute to the central question "What makes one violin better than another?" The first is the "richness" or "beauty" of the sound produced by the violin, and the second is the "playability" of the violin, the ease with which an acceptable note may be produced. The first of these relies, elusively, on the subjective opinion of the listener. However, the distinctiveness of Helmholtz motion makes the second, "playability", more readily amenable to quantitative study: Helmholtz motion either is or is not produced by a given bowing gesture, and if it is, it takes a specific amount of time to become established. The reduction of "playability" to these simple terms means that theoretical models of the bowed string could be used to explore what makes some instruments easier to play than others. Such knowledge would help makers of violins (or indeed of strings, bows, or rosin) to make more "playable" instruments.

This paper will review the present state of knowledge about the mechanics of a bowed violin string, as researchers work towards the goal of a detailed, experimentally validated model which could be used for the kind of design studies just indicated. (The word "violin" is used throughout as a shorthand to include all other members of the family of bowed-string instruments.) The emphasis of this paper will be on the current understanding of the physics of bowed-string instruments, with the aim of answering questions raised by players or makers of acoustic instruments. The modelling developed initially for this purpose has also been applied to real-time synthesis for musical performance purposes, and this has led to a significant research literature with rather different goals and priorities: for a recent review of this work see Smith [2]. These developments will not be discussed in any detail here.

2. The development of theoretical models

2.1. Early work

Helmholtz wrote that "No complete mechanical theory can yet be given for the motion of strings excited by the violin bow, because the mode in which the bow affects the motion of the string is unknown" [1]. Attempting to rectify this situation, Raman [3] was the first to try to describe the dynamics of bowed-string vibration. Working long before the computer age, Raman made several assumptions in order to obtain a model for the motion of the string sufficiently simple to solve by hand. Raman's model is based on a perfectly flexible string, stretched between terminations having reflection coefficients less than unity, excited by a friction force applied at a single point an integer fraction of the string length away from the bridge. The coefficient of friction was assumed to be a function of relative sliding speed between bow and string. Using this model
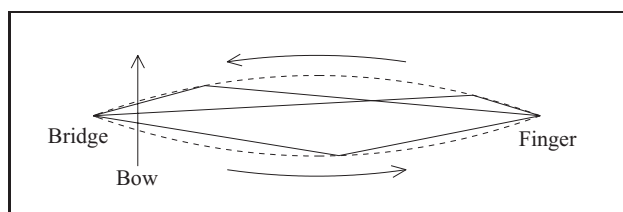
Figure 1. The Helmholtz motion of a bowed string. The dashed line shows the envelope of the motion, and the solid lines show three different snapshots of the string position at different stages in the cycle. The "Helmholtz corner" circulates as indicated by the arrows.

Raman was able to find various possible periodic string motions, including Helmholtz motion.

Some decades later, Friedlander [4] and Keller [5] studied the same model as Raman but with rigid string terminations, and found the surprising result that all periodic waveforms are unstable under those conditions. This obviously conflicts with the experience of playing a real violin. The source of the instability was later tracked down to the absence of dissipation in their model: if an ideal Helmholtz motion is initiated on the string and then a small perturbation is made to it, the perturbation grows with time in the form of a subharmonic modulation of the Helmholtz motion [6, 7, 8]. Although traces of these subharmonics can occasionally be observed in a real bowed string [9], under normal circumstances the energy losses in the string and violin body are sufficiently great that stable periodic motion is indeed possible. The need to allow for losses in a realistic way led to the next major development in modelling.

2.2. Rounded corners and the digital waveguide model

In practice, the perfectly sharp-cornered waves which are a feature of ideal Helmholtz motion, and of Raman's theory, are unlikely to occur. The idea of modifying Helmholtz motion by "smoothing out" the sharp corner was first explored by Cremer and Lazarus [10]. Cremer then studied the change in shape undergone by a rounded corner as it passes underneath the bowing point, and developed an approximate theory of periodic Helmholtz-like motion which showed that the "corner" is significantly rounded when the normal force exerted by the bow on the string is small, but becomes sharper when the force is increased [11, 12, 13]. A sharper Helmholtz corner implies more high-frequency content in the sound, so this gave a first indication of how the player can exercise some control over the sound spectrum of the note: ideal Helmholtz motion is completely independent of the player's actions, except that its amplitude is determined by the bow speed and position.

Cremer's approach was extended to cope with transient motion of the string by McIntyre *et al.* [14, 15], to give what is now usually called the "digital waveguide model" of bowed-string motion. (Similar models were also developed for other self-sustained musical instruments, such as wind instruments [15]. For a recent overview, see [2].) Re-
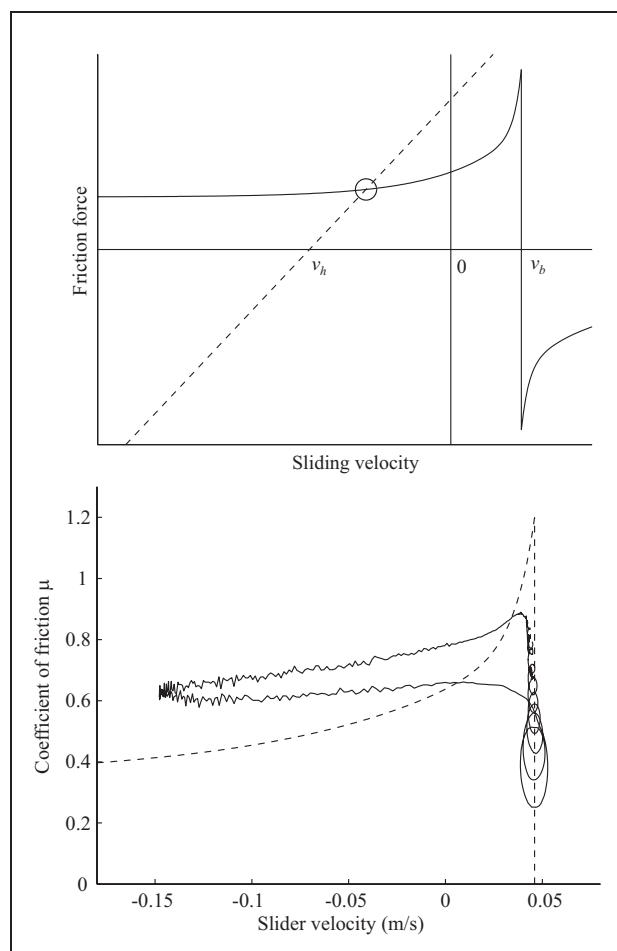

Figure 2. Friction force versus string velocity. (a) The relation assumed by the "friction curve model" (solid line), with a bow speed v_b. The dashed line corresponds to equation (1) as described in the text. (b) The results measured in a dynamic experiment (solid line), showing a hysteresis loop which is traversed in the anticlockwise direction. The dashed line shows the measured result from a steady-sliding test; the bow speed was 0.042 m/s, as indicated by the vertical dashed line. The "sticking" portion of the dynamically-measured curve shows "loops" because the measuring sensor was not exactly at the bow-string contact point [25].

taining for the moment the assumption that the "bow" acts at a single point on the string, two dynamical quantities enter the digital waveguide model: the velocity $v(t)$ of the string at the bowed point, and the friction force $f(t)$ acting at that point. These two quantities can be related to each other in two different ways, which when combined give a complete model.

The first relation between f and v is via the constitutive law governing the friction force. The simplest law, and the one used in all work on the subject until recently, is to assume a nonlinear functional relationship between f and v, of the general form shown in Figure 2a. When the string's velocity matches that of the bow (v_b) the two are sticking, and the force can take any value on the vertical portion of the curve, between the limits of static friction. When

there is relative sliding between string and bow, the friction force falls with increasing sliding speed.

The second relation comes from the vibration dynamics of the string. A force $f(t)$, whether it is applied by a bow or by some other transducer, will excite a particular motion of the string, leading to a particular response $v(t)$ at the driven point. For an ideal string which is *infinitely long*, the applied force would generate a velocity which was simply proportional to the force. Waves would be radiated symmetrically outwards in both directions along the string, and never return. On a finite string, the same outgoing waves are generated, but the velocity response at the bow will have an additional component due to returning reflections arriving back from the ends of the string. In total,

$$v = \frac{f}{2Z} + v_h, \qquad (1)$$

where $Z = \sqrt{Tm}$ is the wave impedance of the string, T is the tension, m is the mass per unit length, and v_h is the velocity contribution due to the returning reflections. The subscript "h" is a reminder that v_h is entirely determined by the past *history* of the motion.

Equation (1) describes a straight line in the f/v plane, with slope $2Z$ and intercept v_h, as indicated by the dashed line in Figure 2a. Since v and f must lie on this straight line, and also on the nonlinear "friction curve", they must therefore lie at the intersection point of the two, ringed in the figure. This graphical view was first described by Friedlander [4] and Keller [5]. The essence of a time-stepping simulation is immediately apparent: at a given time step, v_h is computed from the outgoing waves generated earlier, new values of f and v are computed via the graphical construction, and new outgoing waves are generated. The process is repeated at the next time step, and so on. All that remains to be described is to how to compute v_h.

One way to compute v_h would be to use the Green's function, or in the language of digital filters an FIR filter: the time history of force could be convolved with the impulse response of the string to give the string velocity. However, the impulse response of a typical string takes several seconds to decay away (easily confirmed by plucking the string of an instrument), so this convolution integral must extend over some hundreds of period-lengths. A far more efficient method was discovered in the 1970s, based on treating separately the waves returning from the two ends of the string. The magnitudes of incoming waves can be calculated by convolving recent outgoing waves with a "reflection function" for the relevant portion of string (i.e. the bridge side or the finger side of the bow). The reflection functions encapsulate all effects of propagation, reflection and dissipation during one trip from bow to bridge and back, or from bow to finger and back. They smooth the waves (i.e. round corners) and delay them by the appropriate travel time. The required convolution integrals are quite short: whereas the Green's function method required convolution with the entire history of the string's

motion, this method only requires the motion from the last period or so, since a wave returning to the bow is subsequently replaced by the next outgoing wave travelling in the same direction.

2.3. Early modelling successes

The earliest versions of this digital waveguide model were developed when the first reasonably cheap minicomputers became available. A number of successes were soon chalked up, as various phenomena which had been previously observed in real bowed strings were reproduced, at least qualitatively, by the computer model.

- Helmholtz motion was produced by the model under some circumstances, and it also gave recognisable versions of many other periodic regimes of bowed-string vibration which had been revealed in earlier experimental work [16, 17, 18].
- Detailed string vibration waveforms showed features seen in experiment, such as "Schelleng's ripples" [6, 11, 13, 19]. These are disturbances to the Helmholtz motion generated by the peaks in friction force that occur during transitions between sticking and slipping. By reflecting repeatedly between bow and bridge, or between bow and finger, these disturbances give rise to a pattern with period βT, where T is the period of the Helmholtz motion and β is the bow-bridge distance as a fraction of the string length. (The qualitative explanation of this effect was first developed by Cremer [11, 13] and Schelleng [19].)
- Broadly plausible initial transients could be simulated [13, 14].
- An explanation was given for the "flattening effect", whereby at high values of the normal force from the bow, the period of the Helmholtz motion can be systematically lengthened so that in musical terms the note "plays flat". The effect is associated with a feature of the "Friedlander graphical construction" of Figure 2a which was ignored in Section 2.2. For a certain range of v_h, the straight line and the friction curve may meet in three places rather than one. It can be shown that the resulting ambiguity is resolved by a hysteresis rule, as one might have guessed, and this hysteresis leads to the flattening effect [13, 14, 20]. With higher normal force, the friction curve is scaled up proportionally so that the ambiguous range of v_h becomes wider, and the effect of hysteresis is correspondingly stronger.
- Successful simulations were shown of a "wolf note", a notorious phenomenon particularly common in the cello. If one tries to play a note whose frequency corresponds to a strong resonance of the instrument body, the resulting string motion may show a cyclical alternation between Helmholtz motion and a different vibration regime in which there are two episodes of slipping per cycle, rather than one. The phenomenon was qualitatively explained by Raman [3], and it was successfully simulated by implementing a bridge reflection function which included the effect of a body resonance [13, 14].

- Alongside these uses of the simulation model to investigate bowed-string physics, the digital waveguide algorithm has also been applied to real-time synthesis for musical purposes: see for example Smith [2].

3. Ingredients of a complete model

The digital waveguide model can be extended to give a rather complete representation of realistic bowed strings, but to do so requires a surprisingly long list of effects to be taken into account.

3.1. String bending stiffness and damping

The transverse vibration dynamics of an ideal flexible string are taken into account by the basic version of the digital waveguide model just described. However, real strings have some bending stiffness, or resistance to curvature, which in the words of Schelleng [19] "endangers the beautiful simplicity of the flexible string". The effects of bending stiffness become increasingly significant as the wavelength decreases, i.e. as frequency increases. In terms of travelling waves, bending stiffness causes wave dispersion such that higher frequency waves propagate along the string faster than lower frequency waves. To allow for this, a more complicated reflection function is needed [21].

In addition, the reflection functions must capture the energy dissipation occurring during wave propagation. A useful first approximation is to attribute "constant-Q" behaviour to the vibrating string, so that (leaving aside for the moment effects due to coupling to the violin body) all vibration modes of the string have the same damping factor. A simple reflection function which approximately achieves this effect was described by Woodhouse and Loach [22]. In reality, the damping behaviour of musical strings is more complicated than this [23], with significant variation with frequency. Such effects could be incorporated into the digital waveguide formalism by using digital-filter design techniques to match the desired behaviour (see e.g. [2, 24]).

3.2. Torsional motion of the string

The friction force from the bow acts tangentially on the surface of the string, and this will inevitably cause it to twist as well as deflect laterally. Torsional string motion is probably not directly responsible for significant sound radiation from the body of the violin. However, the conversion of transverse waves to torsional waves, which are relatively highly damped [22], may account for a significant part of the energy dissipation during bowing. In turn, this torsional energy dissipation may help to suppress "Friedlander's instability" [4, 5, 8, 10] mentioned earlier. On the basis of measurements of the torsional impulse response of a selection of cello strings, Woodhouse and Loach suggested that constant-Q behaviour was an adequate model for torsional damping [22].

The digital waveguide simulation model can readily be extended to include torsion. The friction force at the bow generates outgoing torsional waves, similar to the outgoing transverse waves. The combined magnitude of incoming waves v_h, for use in equation (1), is now given by the sum of the velocities of the two incoming transverse waves, already described, plus the corresponding string-surface linear velocities resulting from the incoming torsional waves from the two ends of the string. Torsional waves will have their own wave speed and reflection behaviour, all of which can be described by suitable reflection functions in much the same way as was done for the transverse waves. Equation (1) is then used as before, except for a reduction in the value of the impedance Z to take account of the combination of wave types [15].

3.3. Coupling to the body

Since the aim is to model playability, it is obviously important to include the effect on the string motion of the vibration of the violin body. Vibration at the string notch of the bridge, and to a lesser extent at the fingerboard, will influence the reflection of transverse waves on the string. This influence is most naturally described in modal terms: each vibration mode of the body will contribute a decaying sinusoidal waveform to the impulse response, and hence to the relevant reflection function [14]. If treated directly these increase the lengths of the convolution integrals which must be carried out to compute the reflected waves. However, it is straightforward to implement this part of the reflection function using a recursive IIR digital filter [24, 25], and thus retain computational efficiency. The modelling of the wolf note, mentioned above, was the first application of this approach.

In the context of synthesis for musical performance purposes, other signal-processing techniques have been developed to deal with body coupling, less accurately than the IIR approach but more efficiently in terms of computation time. Examples are "commuted synthesis" (e.g. [26]), and the use of digital-waveguide meshes to model the body vibration directly [27]. Another alternative modelling strategy, related to the latter, is to represent the entire system of a string coupled to an instrument body by finite-difference or finite-element methods, see e.g. [28].

3.4. Dynamics and finite width of the bow

The ribbon of hair in a real bow has a finite width, as well as some degree of compliance. The first fact means that the bow contacts the string at a range of points rather than at a single point. The second means that the friction force will stretch the hair somewhat so that the velocity given by the player to the bow-stick is not quite the same as the velocity of the bow-hair at the contact with the string. The main effect of finite bow width was first pointed out by Raman [3]: during Helmholtz motion "while it is possible for a single point on the string to have absolutely the same velocity as the bow during every part of its forward motion (i.e. during sticking), kinematical theory shows that it is not possible for every element on a finite region to have absolutely the same velocity as the bow in every part of its forward motion." The reason is that the portion of
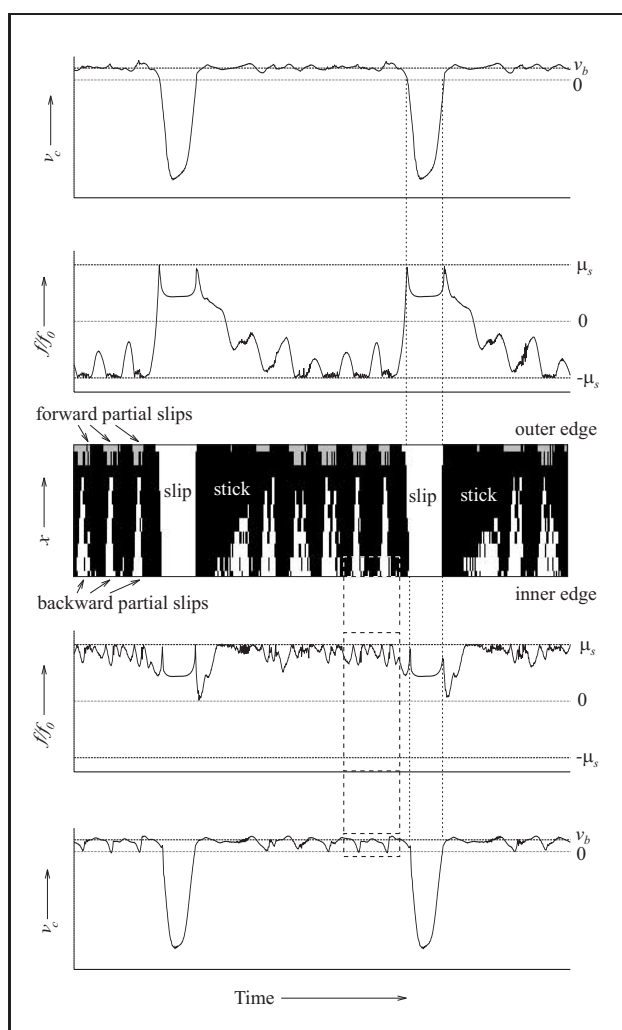
Figure 3. Helmholtz motion simulated using a model including finite bow width and bow-hair compliance, reproduced from [30]. The top and bottom traces represent the string centre-line velocity at the outer and inner edges of the bow, respectively. The adjacent traces show the friction force normalised by the bow force at the same edges. The central plot is a friction map showing the distribution of stick and slip across the width of the bow.

string under the finite-width bow must rotate during sticking (relative to the position assumed in ideal Helmholtz motion). This rotation generates additional friction forces at the edges of the bow, which may become high enough for localised slipping to occur.

McIntyre *et al.* [6] undertook the first serious exploration of this "kinematical" incompatibility and its effects on the motion of the string. For simplicity, they studied the case where the bow contacts the string at two discrete points, and found that slipping was prone to occur at the contact nearer the bridge while sticking continued at the other contact. The resulting irregular vibration of the string between the bow and the bridge produces a characteristic "fuzzy" sound from the violin, especially when played with the bow close to the bridge.

A more comprehensive analysis of the effects of a finite width bow-string contact patch was subsequently pre-

sented by Pitteroff and Woodhouse [29, 30, 31], who in the same analysis included the influence of bow hair compliance. They developed a numerical approach in which the portion of string under and near the bow was treated by a finite difference method, while the waves travelling to and from the ends of the string (outside the finite difference region) were still evaluated using the method of reflection functions. An example of their results is reproduced in Figure 3. This illustrates various aspects of a simulated Helmholtz motion. The central panel of the plot shows the time history of sticking (black pixels) and slipping (white pixels) across the width of the finite bow. Above and below this are waveforms of string velocity and friction force at the two edges of the bow. The phenomenon of localised slipping, anticipated by Raman, is clearly visible.

3.5. The frictional behaviour of rosin

The theoretical concepts described up to this point have been reasonably well corroborated by experimental results, with the exception of the assumption that the friction of rosin (the substance invariably used to coat the hairs of a violin bow to give favourable frictional behaviour) is determined entirely by the relative sliding velocity, in the manner sketched in Figure 2a. Until recently, all published work on the bowed string has assumed this "friction curve model". Numerical values have been given by Lazarus [32] and Smith and Woodhouse [25], who measured the coefficient of friction between two rosined surfaces in a steady sliding apparatus. In such an experiment, friction can only depend upon relative sliding speed. However, in the context of stick-slip vibration there is no reason to dismiss the possibility that other state variables might also influence the tribological behaviour of rosin.

Confirming this suspicion, evidence has been reported recently to demonstrate that the friction coefficient is indeed dependent upon variables other than relative sliding speed. Smith and Woodhouse [25] measured the friction and relative sliding speed between a rosined rod and a vibrating cantilever system, and found that the path traced out in the friction-velocity plane shows a hysteresis loop, no part of which lies close the curve measured in the steady-sliding experiments. An example is reproduced in Figure 2b. Later, Woodhouse *et al.* [33] reported similar results from an apparatus using a bowed string. The friction force and velocity at the bowed point were deduced by inverse computation from measurements of the forces exerted on the two terminations of the string. The conclusion is that although the linear elements of the bowed-string simulation model are believed to perform reasonably well, there is a clear need for a better model for the frictional behaviour of rosin.

A strong candidate for an additional variable controlling the friction of rosin is the *temperature* in the contact region [25, 34]. Rosin is close to its glass transition point at room temperature, so that its mechanical properties change sensitively with small elevations of temperature. Hysteresis in the friction-velocity plane, in qualitative agreement

with the observations, might perhaps be explained by the following repeating sequence of events:

a) When slipping starts, heat is generated at a rate equal to the product of friction force and relative sliding velocity. This heat rapidly raises the local temperature of the rosin, reducing the shear strength and hence the coefficient of friction.

b) After a while, the dynamics of the vibrating string cause the relative sliding velocity to diminish, and hence sticking to re-commence. However, the rosin is still relatively hot from the heat generated during slipping, and so the friction coefficient at the start of sticking is still low.

c) During sticking no heat is generated, and heat is conducted away from the bow-string contact patch. This allows the rosin to cool down, and the shear strength to rise.

The heat generated in the bow/string contact region through friction is counterbalanced by three effects: heat conduction into the material of the bow and string, absorption due to the rate of change of temperature at the contact, and advection as cold rosin enters one side of the contact region while warmed rosin leaves the other side. All these effects can be modelled, approximately at least, quite straightforwardly [25, 34]. The resulting equation for thermal evolution can be implemented in time-stepping simulations, by substituting the relevant terms with finite difference representations. Thus the simulation model of bowed-string motion can be augmented with a parallel calculation of the contact temperature.

It remains to devise a model for how the friction force at the bow-string contact might be influenced by the temperature. Two very simple models have been explored [25]: the "thermal viscous model" and the "thermal plastic model". In the first of these, the rosin is assumed to behave like a viscous liquid whose viscosity decreases as temperature increases. In the thermal plastic model, the rosin is treated as a perfectly plastic solid, which will only deform (i.e. allow slipping) once the shear stress reaches the shear yield strength, which is assumed to be temperature-dependent. For both models, it is possible to choose values for the various parameters (contact size, viscosity or yield strength as a function of temperature, etc.) so as to give results consistent with the measurements in steady sliding tests [25].

Simulations of the bowed-cantilever experiment of Smith and Woodhouse [25] suggested that, of the two, the plastic model produces more realistic-looking stick-slip results than the viscous model. Furthermore, the plastic thermal model predicts hysteresis in the friction/velocity plane similar to that seen in the measurements described above. The conclusion is that the thermal plastic model offers, at the very least, a promising alternative to the old friction-curve model. In section 5, recent work will be described in which the predictions of old and new models were compared with detailed measurements from a bowed cello string to assess whether either model can in fact give accurate predictions under conditions relevant to musical performance.

3.6. Gestural input from the player

Before fully realistic simulations can be performed, it is necessary to know what precisely are these "conditions relevant to musical performance". Studies by Askenfelt [35, 36] have provided some answers to this question. Using an instrumented bow, information was collected on the normal force, bow speed, and bow-bridge distance used by violinists during a variety of different bowing tasks within the normal playing repertoire. As well as giving useful numerical values for input to simulation studies, the results shed light on the complex interactions between these parameters as players strive to achieve particular musical effects. Even if the simulation model were perfect in its representation of the physics of friction and string vibration, it would probably only yield good musical results when "played" with imposed bow gestures embodying some of this subtle interplay. A study by Guettler and Askenfelt [37] on spiccato bowing reinforces this idea: they were able to achieve a reasonably good simulation of this "bouncing bow" technique only by including some subtle details of the phase relation between different components of the player's hand gesture.

A related question about players' gestural control concerns an idea suggested in the Introduction, that "playability" might be somehow quantified in terms of the length of transient before the Helmholtz motion is established on the string. Another study by Guettler and Askenfelt [38] gives data to help define an "acceptably short" transient. Results of two tests were reported. First, musically-trained listeners were asked to rate the sounds of various bowed transients produced by a mechanical bowing machine, and the results correlated with analysis of the transient details of the notes. In the second task, professional violinists were asked to play scales and short musical passages, without being told the purpose of the study, and the transients they produced were analysed. Both parts of the study showed that length of "pre-Helmholtz" transient is indeed a matter of critical importance for good violin sound. Listeners have a narrow and well-defined "acceptance band" for transient length, around 50 ms. Under a range of different bowing conditions the professional players almost invariably produced transients within this acceptance range, including a significant proportion of "perfect transients" in which Helmholtz motion was established essentially from the first cycle. Learning bowing gestures which produce short transients is obviously a significant goal of the long hours of practice needed to master the violin.

4. Mapping parameter space: the Guettler diagram

In order to test whether the simulation model has become sufficiently accurate to give predictive answers about differences of playability, it is necessary to explore its ability to reproduce details of transients in response to a wide range of bow gestures. It is not good enough to look at a single transient: the models contain enough parameters

that one can often "fine tune" them to get a reasonable match to any particular transient. What must be done is to establish suitable *families* of gestures to study, and to perform experiments and simulations using the same families so that detailed comparisons can be made.

The wide range of bowing gestures used by violinists occupy a multi-dimensional parameter space. For the purposes of simulation studies, a sub-family of these gestures must be chosen. In order to plot the results in the form of pictures which can be readily interpreted, the most convenient choice is a two-parameter family of gestures. Various choices were tried in early simulation studies [39, 40, 41], but the example to be used here for illustrative purposes is more recent. Coming to this subject as a player, Guettler [42] pointed out that the "switch-on" transients upon which much of the early computer simulation work was based cannot be achieved in practice: either the bow force or the bow speed (or both) must start from zero. In a "string crossing" or a bouncing bow stroke, the initial bow speed is non-zero but the force increases from zero as the bow comes into contact with the string. For most other bowing attacks, in which the bow is in contact with the string before the stroke starts, the force may be initially non-zero but the bow velocity increases from zero. With this in mind, Guettler proposed that an interesting two-parameter family of bow gestures for study are those having constant bow force, and bow velocity which starts at zero and accelerates at a constant rate. Different gestures in this family can be plotted at different points in the force/acceleration plane.

Guettler performed computational bowed-string simulations, and plotted the time taken to achieve Helmholtz motion at a grid of points in this force/acceleration plane. He also sought analytical expressions for the upper and lower bounds of the regions of this plane containing "perfect transients", combinations of force and acceleration which produce Helmholtz motion without any delay whatsoever. Guettler derived four necessary conditions for the production of a perfect transient, given the same set of simplifying assumptions used earlier by Raman: the effects of wave dispersion or other sources of "corner rounding" were ignored, the ends of the string were treated as dashpots, torsional motion was ignored, the effect of temperature on rosin was ignored, the bow was assumed to contact the string only at a point, the bow hair was assumed to be rigid, and finally the bowing position was required to be an integer division of the string length.

To understand Guettler's four conditions, it is necessary to follow the sequence of events in the first few period-lengths of a theoretical "perfect transient", following a similar approach to the problem by Cremer [43]. Figure 4 illustrates in schematic form the early stages of a perfect transient:

a) Before the first slip, the bow pulls the string outwards quasi-statically.

b) The first time the string slips, two waves (labelled "1" and "2") are sent outwards from the bowing point.
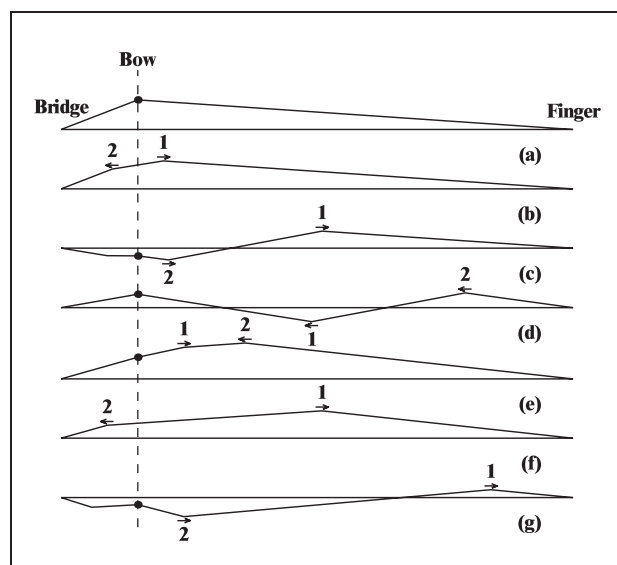

Figure 4. Schematic plots of the string displacement during early stages of a "perfect transient", as described in the text. A black dot at the bowed point indicates when sticking is occurring.

c) The first slip ends when wave 2 passes the bowing point after reflecting from the bridge. Waves 1 and 2 are then both travelling away from the bow towards the finger.

d) Waves 1 and 2 are both inverted when they reflect at the finger, and travel back towards the bow.

e) Wave 1 has the wrong sign to induce slipping, and hence reflects off the (sticking) bow.

f) Wave 2 is however of the same sign as a "Helmholtz corner", and induces slipping when it reaches the bowing point. Hence, while wave 1 continues to travel away from the bow towards the nut, wave 2 travels past the bowing point towards the bridge.

g) The second slip ends when wave 2 passes back over the bowing point. Because wave 1 reflected off the bow whereas wave 2 travelled the extra distance to the bridge and back, the two waves are now wider apart than at stage (c).

h) The sequence continues in a similar way, the two waves getting progressively further apart.

Guettler identified four potential pitfalls in this chain of events:

A) During stages (c) and (d), the friction force required from the bow increases steadily until wave 1 meets the bow, at which point it drops. The first pitfall is hence that the bow force must be sufficient to supply this peak level of friction.

B) The second slip should be induced when wave 2 meets the bow between (e) and (f) above; the second potential pitfall is therefore that the bow force must be low enough that wave 2 can overcome static friction and transmit past the bowing point.

C) Each time wave 2 passes the bowing point the separation between the two waves increases by a distance $2\beta L$ where L is the string length and β is the frac-
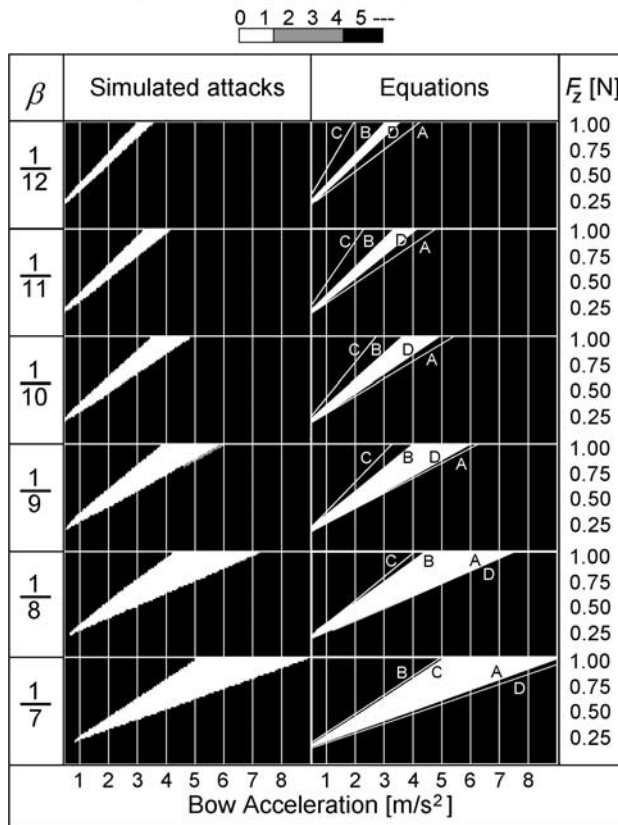
Figure 5. Predicted and simulated regions in the force / acceleration plane where "perfect transients" are possible, reproduced from [42]. Right-hand column: the lines labelled 'A', 'B', 'C', 'D' correspond to the four conditions described in the text. The white wedge shows the region satisfying all four conditions. Left-hand column: results of simulations covering the same parameter space, shaded according to length of pre-Helmholtz transient so that white pixels correspond to perfect transients. The six rows show results for different values of bow position β.
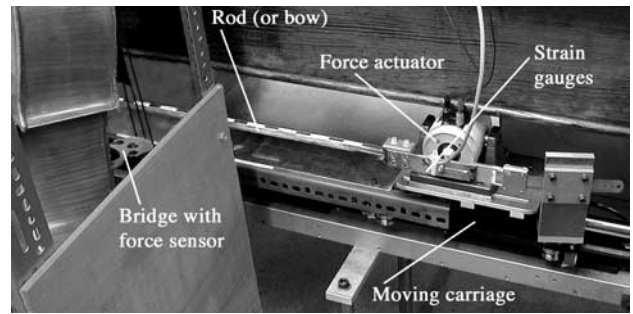

Figure 6. Computer-controlled bowing machine, in this case fitted with a rosin-coated perspex rod to bow a cello.

low frequency strings (such as the C string of a cello or any string of a double bass), almost any interruption to the regular stick-slip pattern of the "perfect transient" is likely to be audible [38]. For such cases perfect attacks must be the player's goal for most bow strokes, and Guettler's conditions provide a guide to what is possible.

The exact formulation of Guettler's four conditions is based on restrictive assumptions, and as such their applicability in practice may be open to question. No doubt, some modifications will occur for more realistic string models: for example, one would expect damping in the string to smooth wave 1 more than wave 2, since wave 2 is "sharpened" each time it passes under the bow [12, 13, 14, 15] whereas wave 1 never passes under the bow, and this will presumably relax the third condition to some extent [42]. Nevertheless, these conditions represent a significant step forward in understanding initial transients, when previous studies had been almost entirely computational in nature and therefore less illuminating as to the governing parameter combinations.

5. Experimental testing

Of course, "Guettler diagrams" like Figure 5 can also be computed using the more realistic bowed-string mdels described in earlier sections. However, before such an exercise can be very convincing, experimental results are needed. In particular, it would be useful to see an experimentally-measured Guettler diagram, which would reveal immediately whether the wedge-like region of perfect transients in Figure 5 gives a useful approximation to real behaviour. Such experiments would also allow detailed comparisons with the predictions of the various models, to show which, if any, predict the behaviour accurately. Eventually, one would hope that such comparisons would lead to the development of a fully validated model with predictive power.

All such experiments require a versatile mechanical bowing machine, because no human player has sufficient control or patience to produce the precise and finely-gradated bowing gestures which make up a Guettler diagram. Such a machine has recently been developed by the authors [44], and is shown in Figure 6. A linear motor carries a bow, or alternatively a rosin-coated perspex

tional distance of the bowed point from the bridge. After a while wave 1 catches wave 2 from behind, and if $1/\beta$ is an integer, they exactly coincide after $1/\beta$ reflections. Bearing in mind that the two waves are of opposite signs, wave 1 tends to cancel wave 2 at this point, so that the slip may not occur: this is Guettler's third pitfall.

D) Finally, Guettler observed that the friction force required from the bow in order to achieve the perfect transient reaches a large value after about $1/3\beta$ reflections of wave 2 from the bridge. This rise in friction may induce a second slip if it reaches the limiting static friction, giving the fourth pitfall.

These four conditions for a perfect attack can all be expressed in simple analytical form, A and D setting minimum levels of bow force while B and C set maximum levels. These predictions were found to agree well with the results of simulations using the Raman-type model, as illustrated in Figure 5 (reproduced from [42]): perfect transients are found in a wedge-shaped region, whose size and position varies with bow position β. Particularly with
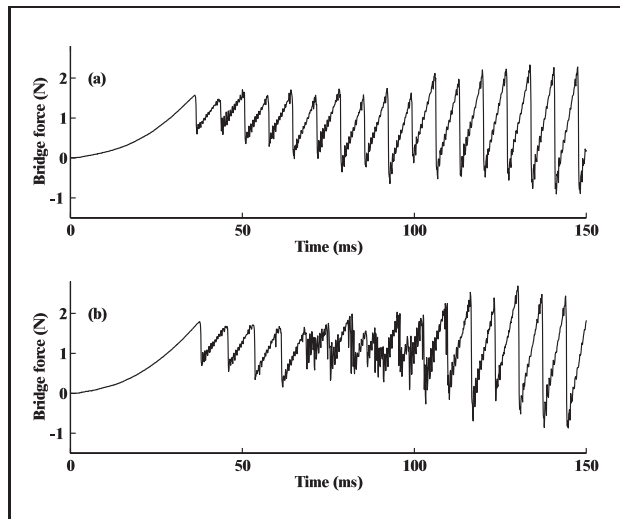
Figure 7. Bridge-force waveforms measured using the bowing machine of Figure 6, using a conventional bow on an open Dominant cello D string (73 Hz). Gestures with constant force and constant acceleration were used, corresponding to points in the Guettler diagram of Figure 8a with pixel coordinates (10,10) and (10,12) respectively.
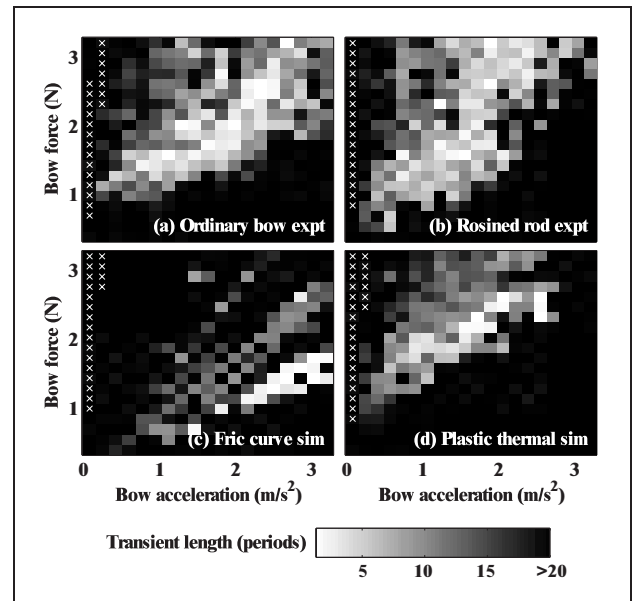

Figure 8. Guettler diagrams, showing length of pre-Helmholtz transient in the force/acceleration plane as described in the text, for an open Dominant cello D string. Top row: measured using the bowing machine, (a) with a conventional bow and (b) with a rosin-coated rod. Bottom row: simulated using (c) the friction-curve model and (d) the thermal plastic model, both assuming a single point of contact between bow and string. All four plots correspond to the same bow position, $\beta = 0.0899$: for (a), this is the position of the centre of the ribbon of bow-hair.

rod (to match more closely the assumptions of simulation models with a single point of contact). The bow position is monitored via a digital encoder which allows a desired trajectory to be tracked by the use of a feedback controller. Similarly, the contact force between the bow and string can be tailored to any desired pattern by another feedback controller, using a force signal from an arrangement of strain gauges in the machine's "wrist", and a force actuator to provide compensatory input. The result is a computer-controlled robot which can produce a wide range of bowing gestures with good accuracy and repeatability. At present the machine cannot cope with "bouncing bow" gestures, but for gestures in which the bow maintains continuous contact with the string it has capabilities comparable with, or better than, a human player [44].

The string motion in response to a given bowing gesture is monitored using a piezo-electric force sensor built into the bridge of the test instrument, a cello in the tests carried out so far. The force sensor is based on a design by Reinicke [45], and responds to transverse force exerted by the vibrating string on the bridge in the plane of bowing. Ideal Helmholtz motion gives a sawtooth waveform from such a sensor, because the transverse force slowly ramps up (or down, depending on the direction of the bow motion) until the moment when the Helmholtz corner reflects from the bridge, when the "bridge force" shows a rapid flyback. Two examples of transients measured in this way, from constant-acceleration bow gestures at two nearby points in a Guettler diagram, are shown in Figure 7. The first shows a perfect attack, in which the sawtooth waveform is established immediately, while the second shows a transient which eventually settles into Helmholtz motion but with a few period-lengths of irregular motion first.

To produce an experimental Guettler diagram the computer is programmed to scan the desired range of force and acceleration, and to capture the string response to each bow stroke. The captured waveforms, like those of Figure 7, are processed automatically by an algorithm which classifies the motion into Helmholtz motion or one of a number of alternative possibilities. For cases which produced Helmholtz motion, the algorithm also determines the length of the pre-Helmholtz transient. The classification algorithm is based on a method originally developed to process the results of simulation studies [34], and it allows "honest" comparisons to be made with simulated Guettler diagrams based on various theoretical models of bowing.

Some results are shown in Figure 8, reproduced from [44]. The top row of this figure shows two measured Guettler diagrams, while the bottom row shows two simulated ones. All four have the same value of β, and the same ranges of bow force and acceleration. Plot (a) shows a measurement using a normal bow, while (b) shows the equivalent measurement using a rosin-coated perspex rod, to give a close approximation to single-point contact with the string. Plot (c) shows simulation results using the friction-curve model based on the best available calibration data for the particular string and rosin used in the experiment. Plot (d) shows simulated results using the thermal plastic model based on the same physical model.

The two measurements both show a wedge-shaped region of "good transients", of the same general form as the

wedge of "perfect transients" predicted by Guettler's analysis and shown in Figure 5. The plots are more "speckly" than Figure 5, showing variation between similar transients at neighbouring points. If the measurement is repeated, the main features remain the same but the details of the speckles change: the bowed string is sufficiently sensitive that even a mechanical bowing machine does not elicit exactly the same transient response from notionally identical bow gestures. The simulated plots also show speckles, but in this case repeated running of the same program will of course produce identical results. The immediate impression from these plots is that the two measurements give similar (but not identical) results, and that the thermal simulation model matches them more closely than does the friction-curve model. The match is far from perfect, and this comparison suggests that the thermal model is on the right lines, but in need of further refinement. That impression is confirmed by more detailed results reported by Galluzzo [44], and research continues to enhance the model in the light of a wide range of experimental results.

6. Conclusions and prospects

Studies of the dynamics of a bowed violin string extend back into the nineteenth century. Models have been developed, especially over the last few decades, to reach a state of some sophistication. It is no exaggeration to say that, at the present time, the motion of a bowed string is the *only* stick-slip oscillation which is reasonably well understood. For other related frictional oscillations, such as squeal in vehicle brakes, theoretical modelling is much less highly developed (see for example the review by Akay [46]). This is not a coincidence. In most engineering problems concerning frictional vibration, and indeed vibration in general, the overriding concern is to understand the behaviour only well enough to design measures which will reduce the vibration and associated noise nuisance. In musical acoustics, things are very different: the essence of music, and in particular of quality judgements by musicians, lies in fine details of vibration and sound. *Any* two violins of reasonable quality are about as similar each other, in terms of measured vibration behaviour, as two nominally identical car bodies coming off a production line. The remarkable range of market values of violins depends on relatively subtle differences of mechanical behaviour.

With this in mind, if a theoretical model of the motion of a bowed string is to be useful for guiding the design of more "playable" instruments, it has to be remarkably accurate. The story which has been summarised in this paper is of the progressive development of a model good enough to do this job. What has been shown is that present-day models are approaching this goal, but that when compared with careful experiments they are not quite up to the task of predicting, reliably, the transient details of the nonlinear response to a given bow gesture. Some parts of the models are probably accurate enough for the purpose, the main uncertainty lying in the constitutive model for the friction force. The wide range of experimental data provided by the recent development of a versatile "bowing robot" gives clues about how the present models are failing, and thus about directions to explore to improve them. There are good grounds for hope that within another decade, a quantitatively accurate model will be developed.

References

[1] H. von Helmholtz: Lehre von den Tonempfindungen. Braunschweig, 1862. English edition: On the sensations of tone, Dover, NY 1954.

[2] J. O. Smith: Digital waveguide modeling of musical instruments. CCRMA, Stanford University, 2003. http://www-ccrma.stanford.edu/jos/waveguide/.

[3] C. V. Raman: On the mechanical theory of vibrations of bowed strings. Indian Assoc. Cult. Sci. Bull. **15** (1918) 1–158.

[4] F. G. Friedlander: On the oscillations of the bowed string. Proc. Cambridge Phil. Soc. **49** (1953) 516–530.

[5] J. B. Keller: Bowing of violin strings. Comm. Pure and Applied Maths **6** (1053) 283–495.

[6] M. E. McIntyre, R. T. Schumacher, J. Woodhouse: Aperiodicity in bowed-string motion. Acustica **49** (1981) 13–32.

[7] G. Weinreich, R. Caussé: Elementary stability considerations for bowed-string motion. J. Acoust. Soc. Amer. **89** (1991) 887–895.

[8] J. Woodhouse: On the stability of bowed string motion. Acustica **80** (1994) 58–72.

[9] R. T. Schumacher: Analysis of aperiodicities in nearly-periodic waveforms. J. Acoust. Soc. Amer. **91** (1992) 438–451.

[10] L. Cremer, H. Lazarus: Der Einfluss des 'Bogendrucks' beim Anstreichen einer Saite. Proc. 6th Int. Congress Acoust., Tokyo, 1968, N–2–3.

[11] L. Cremer: Das Schicksal der 'Sekundärwellen' bei der Selbsterregung von Streichinstrumenten. Acustica **42** (1979) 133–148.

[12] L. Cremer: Der Einfluss des "Bogendrucks" auf die selbsterregten Schwingungen der gestrichenen Saite. Acustica **30** (1974) 119.

[13] L. Cremer: The physics of the violin. MIT Press, Cambridge MA, 1985.

[14] M. E. McIntyre, J. Woodhouse: Fundamentals of bowed-string dynamics. Acustica **43** (1979) 93–108.

[15] M. E. McIntyre, R. T. Schumacher, J. Woodhouse: On the oscillations of musical instruments. J. Acoust. Soc. Amer. **74** (1983) 1325–1345.

[16] O. Krigar-Menzel, A. Raps: Über Saitenschwingungen. Ann. Phys. Chem. (later Ann. Phys. Leipzig) **44** (1891) 623.

[17] B. Lawergren: On the motion of bowed violin strings. Acustica **44** (1980) 194–206.

[18] B. Lawergren: Harmonics of s motion on bowed strings. J. Acoust. Soc. Amer. **73** (1983) 2174–2179.

[19] J. C. Schelleng: The bowed string and the player. J. Acoust. Soc. Am. **53** (1973) 26–41.

[20] X. Boutillon: Analytical investigation of the flattening effect. J. Acoust. Soc. Amer. **90** (1991) 754–763.

[21] J. Woodhouse: On the playability of violins. Part I: reflection functions. Acustica **78** (1993) 125–136.

[22] J. Woodhouse, A. R. Loach: The torsional behaviour of cello strings. Acustica – acta acustica **85** (1999) 734–740.

[23] C. Valette: The mechanics of vibrating strings. – In: Mechanics of Musical Instruments. A. Hirshberg, J. Kergomard, G. Weinreich (eds.). Springer-Verlag, Vienna, 1995.

[24] J. G. Proakis, D. G. Manolakis: Digital signal processing. Prentice-Hall, New Jersey, 1996.

[25] J. H. Smith, J. Woodhouse: The tribology of rosin. J. Mech. Phys. Solids **48** (2000) 1633–1681.

[26] M. Karjalainen, J. O. Smith: Body modeling techniques for string instrument synthesis. Proc. Int. Computer Music Conf., Hong Kong, 1996, 232–239.

[27] P. Huang, S. Serafin, J. O. Smith: A 3D waveguide mesh model of high-frequency violin body resonances. Proc. Int. Computer Music Conf., Berlin, 2000, 86–89.

[28] G. Derveaux, A. Chaigne, P. Joly, E. Bécache: Time-domain simulation of a guitar: model and method. J. Acoust. Soc. Amer. **114** (2003) 3368–3383.

[29] R. Pitteroff, J. Woodhouse: Mechanics of the contact area between a violin bow and a string, Part I: reflection and transmission behaviour. Acustica – acta acustica **84** (1998) 543–562.

[30] R. Pitteroff, J. Woodhouse: Mechanics of the contact area between a violin bow and a string, Part II: simulating the bowed string. Acustica – acta acustica **84** (1998) 744–757.

[31] R. Pitteroff, J. Woodhouse: Mechanics of the contact area between a violin bow and a string, Part III: parameter dependence. Acustica – acta acustica **84** (1998) 929–946.

[32] H. Lazarus: Die Behandlung der selbsterregten Kippschwingungen der gestrichenen Saite mit Hilfe der endlichen Laplacetransformation. Doctoral dissertation, Technical University of Berlin, 1972.

[33] J. Woodhouse, R. T. Schumacher, S. Garoff: Reconstruction of bowing point friction force in a bowed string. J. Acoust. Soc. Amer. **108** (2000) 357–368.

[34] J. Woodhouse: Bowed string simulation using a thermal friction model. Acustica – acta acustica **89** (2003) 355–368.

[35] A. Askenfelt: Measurement of bow motion and bow force in violin playing. J. Acoust. Soc. Amer. **80** (1986) 1007–1015.

[36] A. Askenfelt: Measurement of the bowing parameters in violin playing. II: bow-bridge distance, dynamic range and limits of bow force. J. Acoust. Soc. Amer. **86** (1989) 503–516.

[37] K. Guettler, A. Askenfelt: On the kinematics of spiccato and ricochet bowing. J. Catgut Acoust. Soc. **3** (1998) 9–15.

[38] K. Guettler, A. Askenfelt: Acceptance limits for the duration of pre-Helmholtz transients in bowed string attacks. J. Acoust. Soc. Amer. **101** (1997) 2903–2913.

[39] J. Woodhouse: On the playability of violins. Part II: minimum bow force and transients. Acustica **78** (1993) 137–153.

[40] R. T. Schumacher, J. Woodhouse: The transient behaviour of models of bowed-string motion. Chaos **5** (1995) 509–523.

[41] R. T. Schumacher, J. Woodhouse: Computer modelling of violin playing. Contemporary Physics **36** (1995) 79–92.

[42] K. Guettler: On the creation of the Helmholtz motion in bowed strings. Acustica – acta acustica **88** (2002) 970–985.

[43] L. Cremer: Consideration of the duration of transients in bowed instruments. Catgut Acoust. Soc. Newsletter **38** (1982) 13–18.

[44] P. Galluzzo: On the playability of stringed instruments. Doctoral dissertation, University of Cambridge, 2004.

[45] W. Reinicke: Die Übertragungseigenschaften des Streichinstrumentenstegs. Doctoral Dissertation, Technical University of Berlin, 1973.

[46] A. Akay: The acoustics of friction. J. Acoust. Soc. Amer. **111** (2002) 1525–1548.